



## Leave-Intercalation Theory and Conductive Mechanism during Charge-Discharge Process for Secondary Battery

By C. Z. Yang

*Shanghai University*

**Abstract-** The source of conductive ions in the charge and discharge process of  $AB_5/\beta\text{-Ni(OH)}_2$ , 2H-graphite/  $\text{LiMeO}_2$  and 2H-graphite/ $\text{LiFePO}_4$  batteries is thought to be provided by the phase transition of positive active materials, so it is called phase transition theory. Through the detailed study of the charge and discharge processes of  $AB_5/\beta\text{-Ni(OH)}_2$ , 2H-graphite/  $\text{Li}(\text{Ni}_{1/3}\text{Co}_{1/3}\text{Mn}_{1/3})\text{O}_2$  and 2H-graphite/ $\text{LiFePO}_4$ , it is found that the source of conductive ions is the de-intercalation of H (nickel-hydrogen battery) and Li (lithium-ion battery) in positive and negative active materials, and the de-intercalation theory is proposed. On this basis, the conductive mechanisms of these three types of batteries are clarified: The directional migration and movement of conductive ions under the action of electric field.

**Keywords:** *hydrogen-nickel battery; lithium-ion battery, phase transition theory, x-ray diffraction, de-intercalation theory, conductive mechanism.*

**GJSFR-A Classification:** LCC: TK2941.D432



Strictly as per the compliance and regulations of:



# Leave-Intercalation Theory and Conductive Mechanism during Charge-Discharge Process for Secondary Battery

C. Z. Yang

**Abstract-** The source of conductive ions in the charge and discharge process of  $AB_5/\beta\text{-Ni(OH)}_2$ , 2H-graphite/  $\text{LiMeO}_2$  and 2H-graphite/ $\text{LiFePO}_4$  batteries is thought to be provided by the phase transition of positive active materials, so it is called phase transition theory. Through the detailed study of the charge and discharge processes of  $AB_5/\beta\text{-Ni(OH)}_2$ , 2H-graphite/  $\text{Li}(\text{Ni}_{1/3}\text{Co}_{1/3}\text{Mn}_{1/3})\text{O}_2$  and 2H-graphite/ $\text{LiFePO}_4$ , it is found that the source of conductive ions is the de-intercalation of H (nickel-hydrogen battery) and Li (lithium-ion battery) in positive and negative active materials, and the de-intercalation theory is proposed. On this basis, the conductive mechanisms of these three types of batteries are clarified: The directional migration and movement of conductive ions under the action of electric field.

**Keywords:** hydrogen-nickel battery; lithium-ion battery, phase transition theory, x-ray diffraction, de-intercalation theory, conductive mechanism.

## I. INTRODUCTION

Colleagues in the chemical community know that the 2019 Nobel Prize in Chemistry is awarded to three scientists who have made great contributions to the research and development of lithium batteries. They are Professor John. Good enough in the University of Texas at Austin, Professor M Stanley Witt in gham in State University of New York, Binghamton, USA, and Professor Akira Yoshino in Nagoya University, Japan. This event itself shows that the invention, development and application of lithium-ion batteries are of great significance in science and technology, social progress and the improvement of human quality of life in today's world.

In the past 20 years, due to the development of mobile phones, electric bicycles and new energy vehicles, countries all over the world attach great importance to the research, development and application of renewable energy, and our country also attaches great importance to the research, development, industrialization and application of lithium-ion batteries.

After retiring in August 1999, from 2003 to 2011, he was invited to return to the Shanghai Institute of Microsystems and Information Technology (former

Metallurgy), Chinese Academy of Sciences, which worked for 26 years (1963-1988). Under the leadership of Professor Xia Baojia, he participated in the study of X-ray diffraction characterization of active materials and the mechanism of charge-discharge, cycle and storage of secondary batteries [including Ni/MH, graphite/  $\text{Li}(\text{Ni},\text{Co},\text{Mn})_2$  and graphite/ $\text{LiFePO}_4$  batteries], and published a series of papers.

In 2011, he left the research group due to his wife's health, but did not give up this meaningful work. Yang Chuanzheng, Lou Yuwan, Zhang Jian, Xie Xiaohua and Xia Baojia published the Chinese version of the monograph «Material characterization and electrode process Mechanism of green Secondary batteries» [31] (Science Press, 2011). In 2022, the English version of «Materials and Working Mechanisms of Secondary Batteries» (Springer and Science Press in Beijing, 2022) [32] was published(See Attached). These research results belong to the research group. Not only five authors, but also many graduate students have made important contributions. Li Xiao-Feng, Li Jia, Liu Hui, Yan Jian, Liu Hao-Han, Li Yu-Xia and Wang Bao-Guo are worth mentioning. This is the result of the interdisciplinary study of electrochemistry, chemical power supply experts working closely with material physics and X-ray analysis experts.

This time, at the invitation of the Global Journal of Science Frontier Research, I would like to introduce the relevant research results to readers with two summary papers, so as to communicate and learn from their international counterparts. one is "The Leave-intercalation theory and conductive mechanism during charge-discharge process for secondary battery", the other is "Study on the mechanism of cycle and storage process of lithium-ion battery".

There has been a classic introduction to how the battery works. However, there are few studies on the chemical and physical behavior and conductive physical mechanism in the process of charge and discharge.

Summarize the relevant experimental results, this paper comprehensively introduces a series of important results of X-ray diffraction studies on the charge and discharge processes of  $AB_5/\beta\text{-Ni(OH)}_2$ , graphite/ $\text{LiMeO}_2$  and graphite/ $\text{LiFePO}_4$  batteries, including the de-intercalation theory of the source of

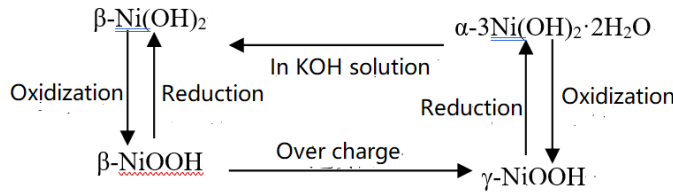


conductive ions in the process of charge and discharge, and then clarifies the physical mechanism of the conductivity of secondary batteries.

## II. EXPERIMENTAL STUDY ON CHARGE AND DISCHARGE PROCESS OF HYDROGEN-NICKEL BATTERY

### a) Phase transition during charge and discharge of hydrogen-nickel battery

In 1966, Bode et al.<sup>[1]</sup> described the working principle of the battery as follows:



The working principle is written as the following chemical reaction formula<sup>[2]</sup>. Positive pole negative pole.



The above description of how the battery works has been written into teaching books and academic monographs<sup>[3]</sup>.

The above tells us that the chemical mechanism of conducting electricity is:

- (1) The  $\beta\text{-Ni(OH)}_2 \rightarrow \beta\text{-NiOOH}$  phase transition occurs during charging, and the  $\text{H}^+$  ion is supplied by this phase transition.
- (2) The transition of  $\text{AB}_5$  hydrogen  $\text{AB}_5\text{H}_x$  (hydride) occurs during the charging process.
- (3) The above two phase transitions are completely reversible in the process of charge and discharge.

The above conductive mechanism can be called phase transition theory. It can also be seen from the above that under the action of electric field, the driving force of  $\beta\text{-Ni(OH)}_2 \rightarrow \beta\text{-NiOOH}$  phase transition is oxidation, and the driving force of  $\beta\text{-NiOOH} \rightarrow \beta\text{-Ni(OH)}_2$  is reduction. It can be seen that oxidation-reduction is for Ni, and oxidation and reduction occur on the positive electrode and discharge respectively, which is not accordance with the principle that oxidation and reduction occur on the positive and negative electrodes respectively during charging (or discharging).

In 1999, Xing Zhengliang, Li Guoxun and Wang Chaoqun reported the results of charge-discharge in-situ XRD observations. The diffraction pattern of 1C charge for 3 h (300%) was identified as the coexistence of  $\beta\text{-NiOOH}$  and  $\gamma\text{-NiOOH}$ . This seems to give the experimental evidence of the conductive phase transition theory of MH/Ni battery. However, the experimental evidence of the coexistence of  $\beta\text{-Ni}$

$\text{OH}^-$  or pure  $\beta\text{-NiOOH}$  phase before fully charged was not obtained. Therefore, it is very necessary to study the physical phenomena and physical conductive mechanism of charge-discharge process in detail, and it also has theoretical and practical significance.

### b) In situ XRD study of $\beta\text{-Ni(OH)}_2$ on Nickel electrode during charging

In this study, the charge in situ observation was carried out by using the charge-discharge in-situ XRD device (patented product) provided by Rigaku Company in Japan. 1C the diffraction patterns of several stages of charging are shown in figure 1. We can see that in the characteristic diffraction spectrum of  $\beta\text{-Ni(OH)}_2$  after 1C charging 50,100,150,480%, only when 1C is 480%, not only the characteristic diffraction pattern of  $\beta\text{-Ni(OH)}_2$ , but also the 003 and 006 diffraction peaks of  $\gamma\text{-NiOOH}$  are observed. The results show that (1) the charge depth of the observed surface is much smaller than that of the interior of the battery, that is, there is a serious hysteresis effect on the surface; (2) in the case of overcharge,  $\beta\text{-Ni(OH)}_2 + \text{-NiOOH}$  coexists rather than  $\beta\text{-NiOOH} + \gamma\text{-NiOOH}$  coexist.

### c) Quasi-dynamic study of positive active material during charge and discharge of MH/Ni battery

The so-called quasi-dynamic is sampling at different stages of charging and discharging, in other words, some stages of charging or discharging of the battery (original, several intermediate and final states) stopped abruptly, and then the battery was dissected

and the positive and negative active materials were obtained as samples for XRD research and analysis.

i. Phase structure change of  $\beta\text{-Ni(OH)}_2$  during charge and discharge of MH/Ni battery

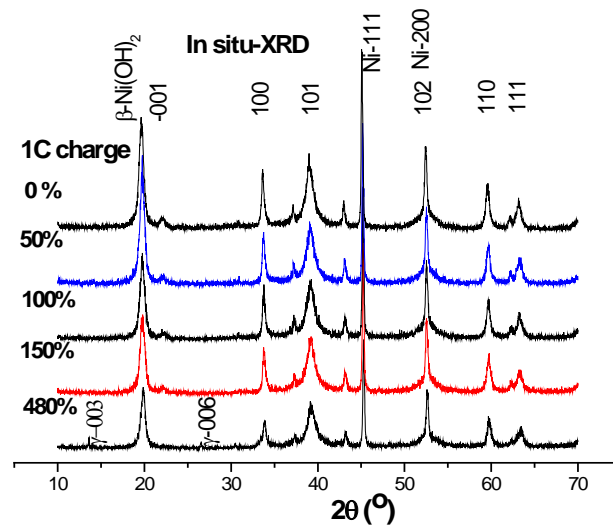


Fig. 1: 1C In situ XRD pattern of  $\beta\text{-Ni(OH)}_2$  at different stages, Cuka

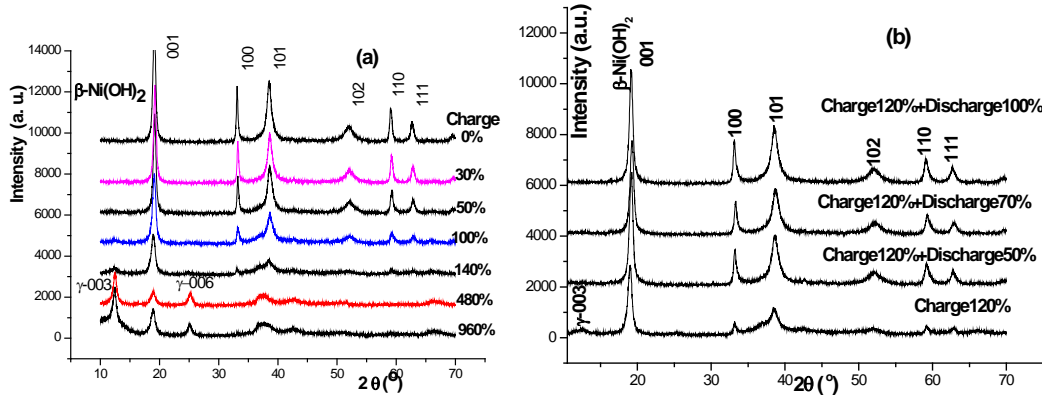


Fig. 2: 0.2c charge (a) discharge (b) XRD spectrum and CuK radiation of positive active material  $\beta\text{-Ni(OH)}_2$  at several stages of charging

Know from figure 2 (a)

- (1) When the charging depth is 0,30,50,100%, the positive active material still belongs to  $\beta\text{-Ni(OH)}_2$ .
- (2) A small amount of  $\gamma\text{-NiOOH}$  is not precipitated until the charging depth reaches 100% and 120%.
- (3) The content of  $\gamma\text{-NiOOH}$  phase increases with the increase of charging depth.

Now let's analyze the 0.2C charging 120% and 140% XRD patterns. The result of 140% charging is shown in figure 3. It can be seen that the positive active material with 140% charge at 0.2C belongs to the mixture of  $\beta\text{-Ni(OH)}_2$  and  $\gamma\text{-NiOOH}$ , rather than a mixture of  $\beta\text{-NiOOH}$  and  $\gamma\text{-NiOOH}$ . Therefore, The pattern of 1C charge for 3 hours (300%) was identified by Xing Zhengliang, Li Guoxun and Wang Chaoqun as the

Figure 2 (a) shows the diffraction pattern of several charging stages.

mixture of  $\gamma\text{-NiOOH}$  and  $\beta\text{-NiOOH}$ , that is worth discussing.

From the relationship (see Fig.4) between  $I_{\gamma\text{-NiOOH-003}}/I_{\beta\text{-Ni(OH)2-001}}$  and overcharge percentage, it can be seen that the content of  $\gamma\text{-NiOOH}$  phase increases with the increase of overcharge percentage.

$\beta\text{-Ni(OH)}_2$  belongs to hexagonal structure, P-3m (No.164) space group. There are 1 molecule, 5 atoms, namely 1 Ni atom, 2 oxygen atoms and 2 hydrogen atoms in the unit cell. The chemical bond between Ni and O is stronger, while that between H and O is much weaker. When there is no stacking disorder, the Ni-O layer presses ABAB .....Stacking in sequence.

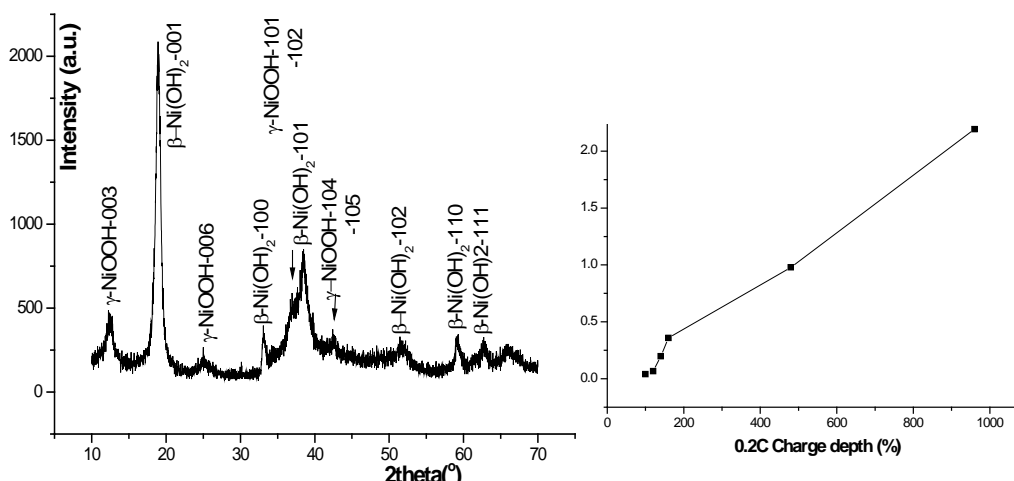


Fig. 3: 0.2 Phase analysis of XRD pattern of cathode chemical material after charging 140%

The experimental results in sections 2.2 and 2.1 have fully proved that there is no phase transition from  $\beta$ -Ni(OH)<sub>2</sub> to  $\beta$ -NiOOH during the charging process of MH/Ni battery. The hydrogen ion H<sup>+</sup> is not provided by this phase transition. The lattice parameters a and c of  $\beta$ -Ni(OH)<sub>2</sub> decrease with the charging process, which indicates that the hydrogen atom leaves the lattice position of  $\beta$ -Ni(OH)<sub>2</sub> and stay a vacancy, which leads to the lattice distortion of  $\beta$ -Ni(OH)<sub>2</sub> and the increase of stacking fault probability. Only when there are enough

hydrogen atoms leaving the  $\beta$ -Ni(OH)<sub>2</sub> lattice for Ni: O: H to fall from 1:2:2 to 1:2:1 does NiOOH precipitate from  $\beta$ -Ni(OH)<sub>2</sub>.

There is now a saying that when  $\beta$ -Ni(OH)<sub>2</sub>  $\rightarrow$   $\beta$ -NiOOH, the volume shrinks by 15%, and when  $\beta$ -Ni(OH)<sub>2</sub>  $\rightarrow$   $\gamma$ -NOOH, the volume shrinks by 18%. This 18% seems to be wrong. When  $\beta$ -Ni(OH)<sub>2</sub>  $\rightarrow$   $\gamma$ -NOOH, the cell volume increases by 262.9% (see Table 1).

Table 1: Related data of  $\beta$ -Ni(OH)<sub>2</sub>,  $\beta$ -NiOOH and  $\gamma$ -NiOOH

Compound	$\beta$ -Ni(OH) <sub>2</sub>	$\beta$ -NiOOH	$\gamma$ -NiOOH
Structure system	Hexagonal	Hexagonal	Hexagonal
PDF card No.	03-0177	06-0141	06-0075
Valence state of Ni	Ni <sup>+2</sup>	Ni <sup>+3</sup>	Ni <sup>+3</sup>
a (Å)	3.126	2.81	2.828
c (Å)	4.605	4.84	20.569
V (Å <sup>3</sup> )	38.97	33.10	141.45
The rate of increase of cell volume (%)	0.00	-15.07	+262.98
Density (g/cm <sup>3</sup> )	3.948	4.62	3.890
Number of molecules / unit cell	1	1	4
V(Å <sup>3</sup> )/ molecule	38.97	33.10	35.36
The rate of change in the volume occupied by a molecule (%)	0.0	-15.0	-9.3

More reasonably, the change in the volume of each molecule in the unit cell should be taken into account. In this way, the cell volume of each molecule is reduced by 15.0% at  $\beta$ -Ni(OH)<sub>2</sub>  $\rightarrow$   $\beta$ -NiOOH and only 9.3% at  $\beta$ -Ni(OH)<sub>2</sub>  $\rightarrow$   $\gamma$ -NOOH, as shown in the last row of table 4. It can be seen that it is more reasonable to have  $\beta$ -Ni(OH)<sub>2</sub> transition  $\gamma$ -NOOH rather than  $\beta$ -Ni(OH)<sub>2</sub> transition  $\beta$ -NiOOH phase transition.

The XRD patterns of several stages in the discharge state are shown in figure 2 (b). We can see that  $\gamma$ -NiOOH has been decomposed, and the phase

structure of  $\beta$ -Ni(OH)<sub>2</sub> has not changed, but their fine structure has changed.

#### ii. $\beta$ -Ni(OH)<sub>2</sub> fine structure [7, 11, 12]

The Refine in the Jade program has been used to determine the peak position and HWHM. The data were processed according to the method of reference [8, 9]. The lattice parameters a and c, the average grain size D<sub>average</sub>, the micro-strain ε<sub>average</sub> and the total stacking fault probability (f<sub>D</sub>+f<sub>T</sub>) of  $\beta$ -Ni(OH)<sub>2</sub> are calculated.

The changing trends in the charge-discharge process are summarized in Table 2.

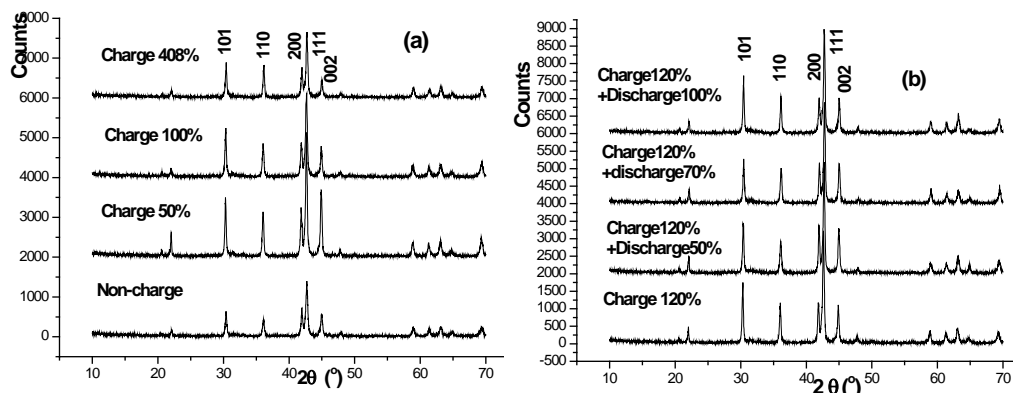
Table 2: Changes of fine structure of  $\beta$ -Ni(OH)<sub>2</sub> during charge-discharge process

Parameter of fine structure		Charge process	Discharge process
Lattice parameter	<i>a</i>	<i>a</i> decrease with the increase of charging depth.	It is roughly opposite to the charging process, but it is not completely reversible.
	<i>c</i>	<i>c</i> Begin to decrease, then increase	
$D_{\text{average}}$		It thinning with the deepening of the charge and discharge process.	
$\varepsilon_{\text{average}}$		With the deepening of the charge and discharge process, it begins to increase, and then becomes smaller.	
$(f_D + f_T)$		With the deepening of the charging process, it begins to increase slowly, and then increases faster.	

d) Quasi-Dynamic study of negative electrode active material AB<sub>5</sub> during charge-discharge process

The XRD spectrum of the negative electrode active material AB<sub>5</sub> in several stages of charge and discharge is shown in figure 5. On the whole, the structure of AB<sub>5</sub> alloy has no obvious change during charging, but the fine structure and microstructure also change. The changing trend with the charge-discharge

process is summarized in Table 3. It can be seen that both *a* and *c* increase with the increase of charging depth, and the micro-strain  $\varepsilon$  also increases with the increase of charging depth. The discharge situation is just the opposite, but it returns to the original state, which indicates that there is some irreversibility in the charge-discharge process.

Fig. 5: XRD diagram of negative electrode active material AB<sub>5</sub> alloy at several stages of charging (a) discharging (b) chargingTable 3: Changes of fine structure of AB<sub>5</sub> alloy during charge-discharge process

Parameter of fine structure		Charge process	Discharge process
Lattice parameter	<i>a</i>	Increase with the deepening of the charging process	It is roughly opposite to the charging process, but it is not completely reversible.
	<i>c</i>	Increase with the deep of the charging process	
Micro-strain $\varepsilon$		Increase with the deep of the charging process	

### III. EXPERIMENTAL STUDY ON CHARGE AND DISCHARGE PROCESS OF 2H-GRAFPHITE/LIME O<sub>2</sub> BATTERY

Lithium-ion battery is a new generation of green high-energy battery developed in the early 1990s, which has the characteristics of high energy density, high working voltage, long cycle life and low self-discharge rate, and has been widely used. It will become the

preferred battery for electric vehicles and hybrid vehicles. As far as positive active materials are concerned, there are mainly four types of positive active materials: LiCoO<sub>2</sub>, Li (Ni, Co)O<sub>2</sub>, Li (Ni, Co, Mn)O<sub>2</sub> and LiFePO<sub>4</sub>, but the negative active materials are all 2H-graphite with hexagonal structure, so there are various systems of 2H-graphite/LiCoO<sub>2</sub>, 2H-graphite/ Li(Ni,Co)O<sub>2</sub>, 2H-graphite/Li(Ni,Co,Mn)O<sub>2</sub> and 2H-graphite/LiFePO<sub>4</sub>. Moreover, there are different proportions in the

binary or ternary systems of  $\text{Li}(\text{Ni},\text{Co})\text{O}_2$  and  $\text{Li}(\text{Ni},\text{Co},\text{Mn})\text{O}_2$ . However,  $\text{LiCoO}_2$ ,  $\text{Li}(\text{Ni},\text{Co})\text{O}_2$  and  $\text{Li}(\text{Ni},\text{Co},\text{Mn})\text{O}_2$  have the same crystal structure, so they can be written as general  $\text{LiMeO}_2$ .

a) *Structural evolution of positive active materials during charge-discharge of 2H-graphite/LiMeO<sub>2</sub> battery*

In 1992, Reimers and Dahn<sup>[14]</sup> used an on-line (in situ) X-ray diffraction device to find that when  $\text{Li}_{x}\text{CoO}_2$  is in the charging process of  $x=0.5$ , due to lattice distortion,  $\text{O}-\text{Li}-\text{O}-\text{Co}-\text{O}-\text{O}..$ , ABCABC... The rhombohedral structure  $R\bar{3}m$  of the stack is transformed into a monoclinic structure; Amatucci et al. (1996)<sup>[15]</sup> considered that the positive terminal of the battery at full charge is  $\text{CoO}_2$ , which has a hexagonal structure. Yang and McBreen et al.<sup>[16,17]</sup> studied the phase transition of  $\text{Li}_{1-x}\text{CoO}_2$  during charging by means of on-line synchrotron radiation X-ray diffraction ( $\lambda = 1.195$ ). It is concluded that  $\text{Li}_{1-x}\text{CoO}_2$  changes into monoclinic M2 phase at  $0.75 < x < 0.85$ , and from hexagonal phase H2 of  $\text{CdCl}_2$ - type to O1A phase of  $\text{CdCl}_2$ - type at  $0.77 < x < 1.00$ , which belongs to P63mc space group. Finally, it becomes O1 phase, which is  $\text{CoO}_2$ . However, these studies only focus on the phase transition of  $\text{LiCoO}_2$  materials during battery charging,

and do not involve the changes of fine structure and microstructure; at the same time, they do not systematically study the fine structure changes of positive and negative active materials in the process of charge and discharge from the point of view of chemical physics. Therefore, in order to deeply understand the structural evolution of electrode materials in the actual battery operation process and explore the working mechanism of electrode materials in the real battery system, this section introduces the use of X-ray diffraction to study the crystal structure and microstructure changes of graphite/ $\text{LiCoO}_2$  and graphite/ $\text{Li}(\text{Ni}_{1/3}\text{Co}_{1/3}\text{Mn}_{1/3})\text{O}_2$  lithium-ion batteries during charge and discharge.

The XRD patterns of the cathode active material  $\text{LiCoO}_2$  at different stages of charge and discharge are shown in figure 6. As can be seen from the figure, in the battery charging process, the change of the (006) peak in the cathode material XRD pattern is the most significant. At the initial stage of battery charging (10% charging), it splits at first, then moves to a low angle as the battery charge state continues to increase, and finally disappears; while other diffraction peaks have no other obvious changes except a small offset.

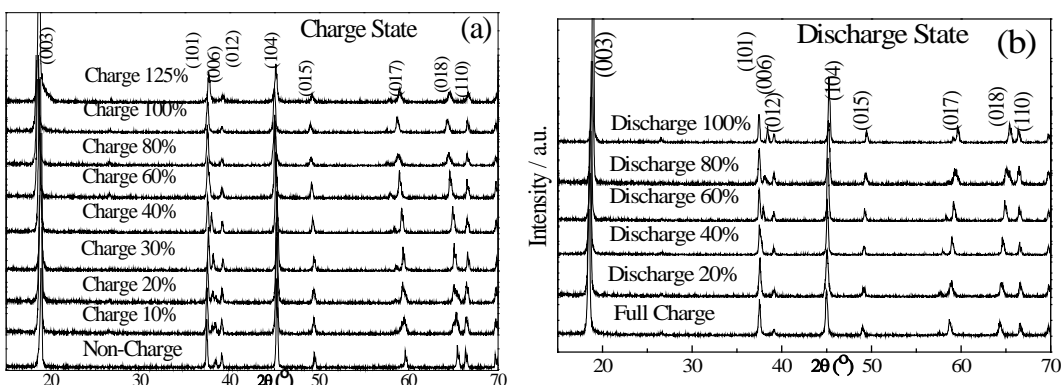


Fig. 6: X-ray diffraction patterns of cathode materials in several main stages of charge and discharge of 18650 graphite/ $\text{LiCoO}_2$  battery

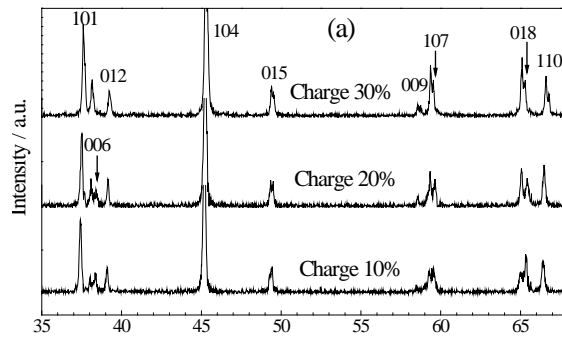


Fig. 7: XRD pattern of cathode material  $\text{LiCoO}_2$  after removal of  $\text{K}\alpha_2$  when the battery is charged at 10%, 20% and 30%.

In order to clearly investigate the structural changes of the cathode material  $\text{LiCoO}_2$  when the

battery was charged by 10% to 30%, the three diffraction patterns were magnified in figure 7 after removing  $\text{CuK}\alpha_2$

components. As can be seen from figure 7, from the battery charge to 10%, in the spectrum (006), The four diffraction peaks of (015), (107) and (018) were all split into two peaks. At the same time, it was found that the intensity of the low angle peak (left peak) was lower than that of the high angle peak (right peak) after the split of each peak (006, 107, 018) at the initial charging stage (10% charging).

As the cell continues to charge (to 20%), the intensity of the low-angle peak increases, the intensity of the high-angle peak weakens, and the intensity of the two peaks is reversed.

The lattice parameters of the two peaks are calculated as two independent phases: when the battery is charged at 20%, the corresponding low-angle peak.

The lattice parameters of the high-angle peak are asides 2.8114, 14.1670, and the high-angle peaks are 2.8104, 14.0983, respectively. It can be seen that the

lattice parameters of the two phases are different, but from the characteristic peak, both phases are still  $\text{LiCoO}_2$  phase.

The above analysis results can be explained as follows: at the initial stage of battery charging (up to 10%), the lattice parameters of the material are changed due to the separation of Li from the  $\text{LiCoO}_2$  lattice, and the  $\text{LiCoO}_2$  lattice parameters of the unde-Li remain unchanged, so there are two phases, which is called the lithium-deficient phase; as the battery continues to charge, with the continuous removal of Li, the relative intensity of the two-phase characteristic peaks reverses, indicating that the content of the lithium-deficient phase increases and the content of the original phase decreases. This clearly shows that the de-Li of  $\text{LiCoO}_2$  has a process from the surface of the electrode to the inner layer.

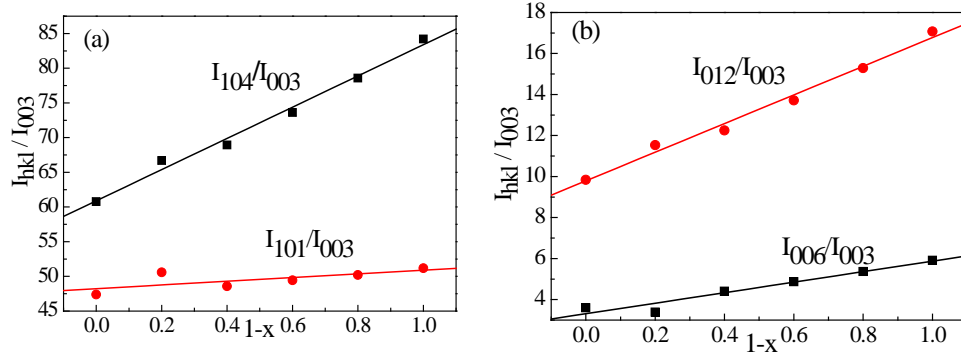


Fig. 8: The relationship between the intensity of the main diffraction lines of  $\text{Li}_{1-x}\text{CoO}_2$  and  $1-x$

At the same time, as can be seen from figure 6 (a), when the battery is charged to 30% or 40%, the positive active material becomes single-phase again.

The data of the standard  $\text{LiCoO}_2$  are roughly consistent, only the lines have some displacement; when the battery continues to charge to 60%, 80%, 100% and 125%, except for the disappearance of 006 lines, the other lines are still consistent with the data of the standard  $\text{LiCoO}_2$ , and no new phase is generated. This is different from the report of McBreen et al. The reasons for the disappearance of 006 lines are as follows:

- (1) The diffraction intensity of 006 decreases due to the removal of Li. For this reason, we use the Power Cell program to calculate the relative intensity of each diffraction line according to the  $\text{Li}_{1-x}\text{CoO}_2$  model. The relationship between the relative intensity of each main diffraction line and  $1-x$  is shown in figure 8. It can be seen that when  $1-x=0$  is used, the diffraction intensity of 006 decreases very low and is not visible.
- (2) It is possible that 006 overlaps with 101 or 012 due to the change of lattice parameters.

- (3) The mixed arrangement of Li/Ni atoms may occur in 2H-graphite/Li $\text{Ni}_{1/3}\text{Co}_{1/3}\text{Mn}_{1/3}\text{O}_2$  battery during charge and discharge<sup>[17]</sup>.

Comparing figs. 8 (a) and (b), it can be seen that the structural change of the positive material  $\text{LiCoO}_2$  during the discharge of the battery is basically the reverse process of charging.

b) *Structural evolution of negative active materials 2H-graphite*

The XRD patterns of 2H-graphite/ $\text{LiCoO}_2$  lithium-ion battery with hexagonal graphite as negative active material during the charge and discharge process are shown in Fig.9(a) and (b) respectively. The results of the analysis are listed in Table 4.

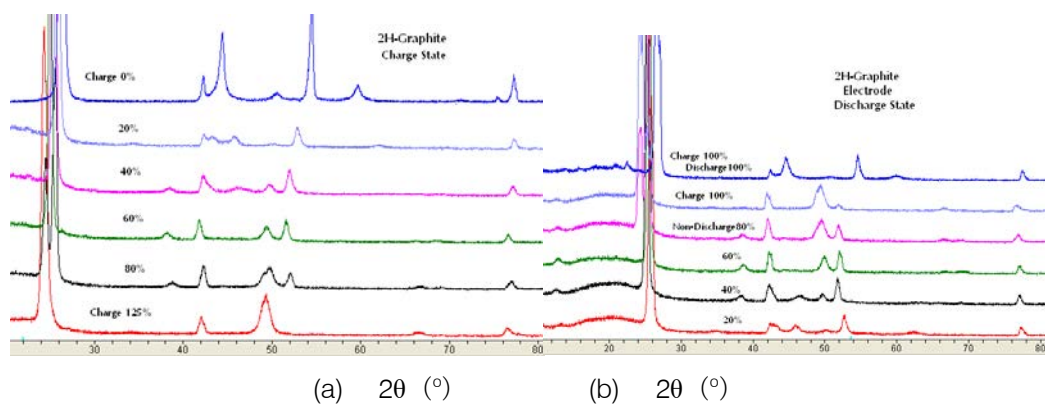


Fig. 9: XRD pattern of negative active materials during charge and discharge of lithium-ion battery. (a) main stages of charging (b) main stages of discharge

Table 4: Results of phase analysis of negative active substances during charge and discharge

Charge state		Discharge state		
charge (%)	Existing phase	discharge (%)	no discharge (%)	Existing phase
0	2H-graphite	100	0	2H-graphite 1+2H-graphite 2
10	2H-graphite 1+2H-graphite 2			
20	2H-graphite	80	20	2H-graphite 1+2H-graphite 2
30	2H-graphite			
40	2H-graphite	60	40	2H-graphite
60	2H-graphite	40	60	2H-graphite +LiC <sub>12</sub>
80	LiC <sub>24</sub> +LiC <sub>6</sub>	20	80	LiC <sub>12</sub> +LiC <sub>6</sub>
100	LiC <sub>6</sub> + Li <sub>2</sub> C <sub>2</sub> + LiC <sub>12</sub> + LiC <sub>24</sub>	0	100	LiC <sub>6</sub> + Li <sub>2</sub> C <sub>2</sub> + LiC <sub>12</sub> + 2H-graphite
125	LiC <sub>6</sub> + Li <sub>2</sub> C <sub>2</sub>			

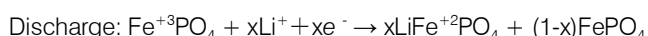
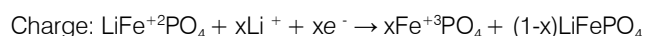
As can be seen from figures 9 and Table 4, there is a gap between the hexagonal grids of carbon atoms embedded in the graphite lattice of Li atoms to form a solid solution, and then Li<sub>C24</sub>, LiC<sub>12</sub>, LiC<sub>6</sub> and Li<sub>2</sub>C<sub>2</sub> are precipitated. As for when these compounds are precipitated, it is related to the system of lithium-ion battery and the ratio of positive and negative active materials.

#### IV. EXPERIMENTAL STUDY ON CHARGE DISCHARGE PROCESS OF 2H GRAPHITE/LiFePO<sub>4</sub> BATTERY

##### a) Phase identification of 2H-graphite/LiFePO<sub>4</sub> battery during charge and discharge<sup>[23]</sup>

LiFePO<sub>4</sub> has become one of the most likely cathode active materials to replace lithium secondary battery<sup>[19]</sup>. This is because lithium secondary ion battery with lithium iron phosphate as cathode has the characteristics of high safety, long life, low cost and environment-friendly, so it has become the focus of development and research in the battery industry. At room temperature, the de-intercalation behavior of LiFePO<sub>4</sub> is actually a two-phase reaction process forming the two-phase interface between FePO<sub>4</sub> and

LiFePO<sub>4</sub>. Newman<sup>[20]</sup>, Yamada<sup>[21]</sup> and Dodd<sup>[22]</sup> have systematically studied the phase transition during the charge-discharge process of LiFePO<sub>4</sub>. During charging, the lithium ion migrates from the FeO<sub>6</sub> layers and enters the negative electrode through the electrolyte, resulting in the oxidation reaction of  $Fe^{2+} \rightarrow Fe^{3+}$ . In order to maintain the charge balance, the electron arrives at the negative electrode from the external circuit. The reduction reaction occurs during the discharge, and the discharge is opposite to the above-mentioned process. However, the oxidation-reduction occurs on the positive electrode and corresponds to charge-discharge respectively. That is:



LiFePO<sub>4</sub> is a typical electron-ion mixed conductor with a band gap of 0.3eV, low electronic conductivity at room temperature and low ionic conductivity at room temperature (about 10~5S/cm). Therefore, in order to use LiFePO<sub>4</sub> as cathode material for lithium-ion battery, it is necessary to improve its

electronic and ionic conductivity and improve its electrochemical interface properties.

Figure 10 shows the X-ray diffraction pattern of the positive plate at several stages of the charging (a) and discharging (b) process, and the Pnma orthogonal

structure can be used to index  $\text{LiFePO}_4$  and  $\text{FePO}_4$ , represented by the letters T and H, respectively. It should be noted that  $\text{FePO}_4$  with orthogonal structure [Pnma (No.62), 34-0134] can only be used for 100% charging patterns,

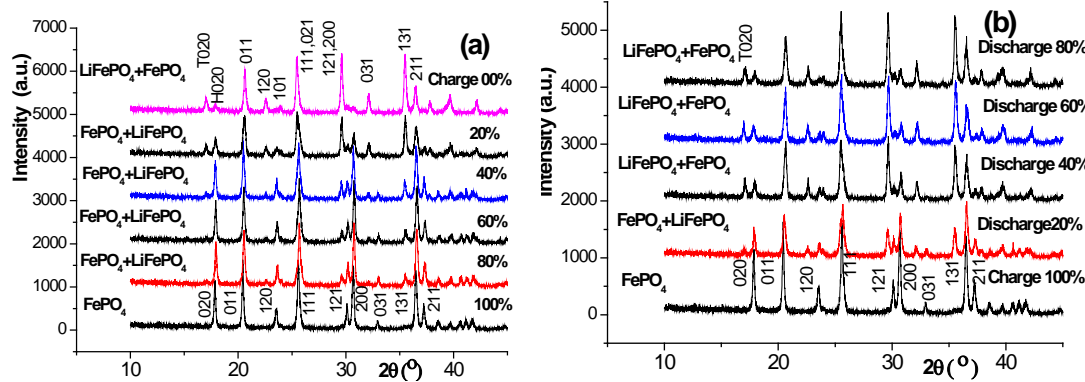


Fig. 10: XRD pattern of positive active material after 0.2C charging (a) and discharging (b) after active 2H-graphite/ $\text{LiFePO}_4$  battery but not other structures [CmcM]

The  $\text{FePO}_4$  of (No.63) or  $\text{P}_{22}2222$  (No.180) is indexed. It can be seen that there are  $\text{LiFePO}_4$  and  $\text{FePO}_4$  in the positive active material after the aforementioned formation, and the content of the former is more. With the increase of the charging depth, the  $\text{LiFePO}_4$  gradually decreases and the  $\text{FePO}_4$  gradually increases. When the charge reaches 80%, there is still a trace of  $\text{LiFePO}_4$ , and it is not all  $\text{FePO}_4$  until the charge reaches 100%.

From the diffraction pattern of several stages of the discharge process [figure 8 (b)], it can be seen that the positive electrode of the fully charged battery is composed of pure  $\text{FePO}_4$ , and  $\text{LiFePO}_4$  appears at 20% discharge, and increases with the increase of discharge depth, until 80% discharge, although it is dominated by  $\text{LiFePO}_4$ , there is still a considerable amount of  $\text{FePO}_4$ . Comparing the phase composition of the positive active material of 80% discharge with that of the positive active material when charging 20%, there is an obvious difference between them, which shows that the positive active material is not completely reversible or called asymmetry in the charge-discharge process, but it indicates that there is a change of  $\text{LiFePO}_4 \leftrightarrow \text{FePO}_4$  in the charge-discharge process.

However, based on the synchrotron radiation online (in situ) XRD method, Shin, Chung and Min et al. [24] found that the asymmetry of structural change was not observed in carbon-coated  $\text{LiFePO}_4$  during 0.2 C charge/discharge, and but the asymmetry became serious when the magnification factor increased to 2C and 10C.

#### b) Quantitative analysis of phase study on the hysteresis effect of discharge

In order to further analyze the asymmetry of the phase transition of the positive active material during the

charge and discharge of graphite/ $\text{LiFePO}_4$  battery, the relative contents of  $\text{FePO}_4$  and  $\text{LiFePO}_4$  in the positive active material at each stage of charge and discharge were quantitatively determined by Zervin's non-standard method [26, 27]. The results are shown in figure 11. As can be seen from figure 9, (1) even in 0%SOC, the positive active material is not entirely  $\text{LiFePO}_4$  phase, in which there is a small amount of  $\text{FePO}_4$  phase (calculated to be about 8%), which is due to the formation of inactive  $\text{FePO}_4$  shell during the first charge. (2) in the case of the same SOC, the content of  $\text{LiFePO}_4$  in the discharge state is more than that in the charge state, on the contrary, the  $\text{FePO}_4$  content in the discharge state is obviously low charge state, which obviously reveals that the asymmetry of charge and discharge is caused by the hysteresis effect of discharge.

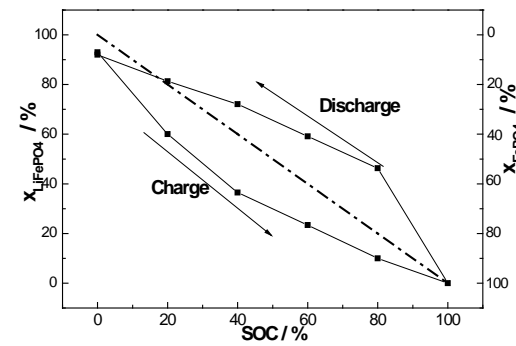


Fig. 11: Content change of  $\text{LiFePO}_4$  and  $\text{FePO}_4$  in positive active materials during charge and discharge of graphite/ $\text{LiFePO}_4$  battery., ——— 45 degree line

#### c) The phase transition nature of $\text{LiFePO}_4 \rightarrow \text{FePO}_4$ [20]

Both  $\text{LiFePO}_4$  and  $\text{Li}_{1-x}\text{FePO}_4$  belong to triphylite orthorhombic system and Pnma (No.62) space group, while  $\text{FePO}_4$  belongs to heterosite orthorhombic system

and can only be indexed by Pnma (No.62) space group. The actual measured lattice parameters are:

	a(Å)	b(Å)	c(Å)	V(Å <sup>3</sup> )	(V <sub>T</sub> -V <sub>H</sub> )/V <sub>T</sub>
LiFePO <sub>4</sub>	6.0157	10.3915	4.7207	295.101	0.00 %
FePO <sub>4</sub>	5.8094	9.9222	4.8166	277.638	- 5.92 %

Each unit cell of crystalline LiFePO<sub>4</sub> contains four LiFePO<sub>4</sub> molecules, namely, 4 Li atoms, 4 Fe atoms, 4 phosphorus atoms and 16 oxygen atoms, with a total of 28 atoms. The atomic position is as follows<sup>[25]</sup>:

	x	y	z	
Li 4a	0	0	0	
Fe 4c	0.282	1/4	-0.023	
P 4c	0.095	1/4	0.418	
O1 4c	0.107	1/4	-0.268	+ 0 1/4 0;1/2 0 1/2;1/2 1/2 1/2
O2 4c	0.460	1/4	0.208	
O3 8d	0.165	0.043	0.288	

The FePO<sub>4</sub> unit cell also contains four FePO<sub>4</sub> molecules, namely, 4 Fe atoms, 4 phosphorus atoms, 16 oxygen atoms, a total of 24 atoms, and their atomic positions are as follows<sup>[26]</sup>

	x	y	z	
Fe 4c	0.277	1/4	0.9449	
P 4c	0.0935	1/4	0.3983	
O1 4c	0.1167	1/4	0.7131	+ 0 1/4 0;1/2 0 1/2;1/2 1/2 1/2
O2 4c	0.4417	1/4	0.1614	
O3 8d	0.1684	0.0461	0.2513	

The crystal structure model and chemical combination of LiFePO<sub>4</sub> and FePO<sub>4</sub> are shown in figs. 12 and 13, respectively.

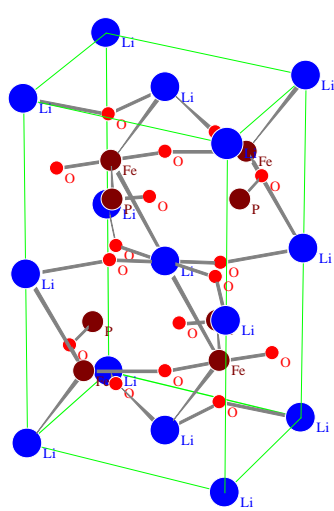


Fig.12: Crystal structure model and bonding of Pnma (No.62) olivine LiFePO<sub>4</sub>

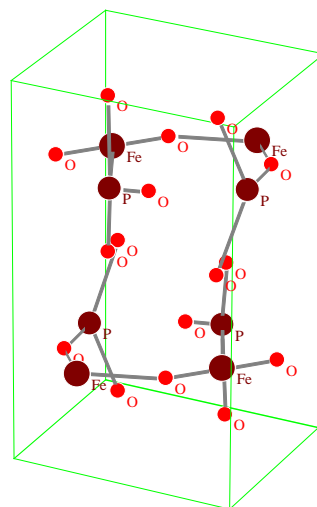


Fig.13: Structural model and bonding of FePO<sub>4</sub> of Pnma (No.62) space group structure

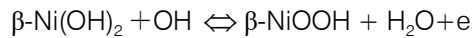
From the structural data of the two substances (including space groups, lattice parameters and atomic positions in the unit cell) and the structural models of Fig. 12 and Fig.13, it is known that the crystal structures of the two substances are almost the same. The change of  $\text{LiFePO}_4 \rightarrow \text{Li}_{1-x}\text{FePO}_4 \rightarrow \text{FePO}_4$  ( $x=1$ ) is not a real structural phase transition, only because the Li atom gradually leaves the 4a position of the  $\text{LiFePO}_4$  crystal lattice under the action of electric field, which changes from  $\text{LiFePO}_4$  to  $\text{Li}_{1-x}\text{FePO}_4$  Lack Li, and then to  $\text{FePO}_4$  without Li. However, the crystal structure remains basically unchanged, but only the crystallographic position of each atom moves slightly. Therefore, the change of  $\text{LiFePO}_4 \rightarrow \text{Li}_{1-x}\text{FePO}_4 \rightarrow \text{FePO}_4$  is not the phase transition of real phase structure change, but can be called pseudo phase transition.

## V. LEAVE-INTERCALATION THEORY DURING CHARGE/DISCHARGE PROCESS FOR SECONDARY BATTERY<sup>[29]</sup>

### a) Comprehensive analysis

On the basis of the above research results, the de-intercalation theory of ionic conductivity of secondary battery and the de-intercalation behavior of positive and negative active materials are described from an overall point of view.

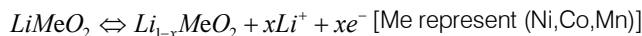
The following reactions do not occur at the positive electrode during the charging and discharging process of the hydrogen-nickel battery.



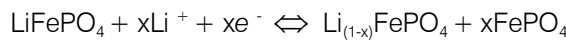
The following reactions occur at the positive electrode of 2H-graphite/ $\text{LiCoO}_2$  lithium-ion battery during charge and discharge.



The following reactions occur at the positive electrode of 2H-graphite/  $\text{Li}(\text{Ni},\text{Co},\text{Mn})\text{O}_2$  lithium-ion battery during charge and discharge.



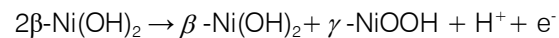
The following reactions occur at the positive electrode of 2H-graphite /  $\text{LiFePO}_4$  lithium-ion battery during charge and discharge.



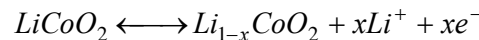
So people come to the conclusion that the conductive ions of the battery are provided by phase transition, which is called the phase transition theory of ionic conductivity.

After careful analysis, it is found that the oxidation reaction occurs at the positive electrode and the reduction reaction occurs at the positive electrode during discharge. in other words, the phase transition force during charging is oxidation reaction, and the driving force during discharge is reduction reaction, but this is not consistent with the following principle. that is, in the process of realizing the direct conversion of chemical energy into electric energy, the chemical power supply is in the process of directly converting chemical energy into electric energy. There must be two necessary conditions, one of which is that the process of losing electrons (oxidation) and obtaining electrons (reduction) in chemical reactions must be separated on positive and negative electrodes. Therefore, it is different from the general oxidation-reduction reaction.

Our experimental study found that: The above phase transition does not occur during the charging process of the hydrogen-nickel battery, and the following phase transition occurs only when the battery is fully charged and overcharged.



Although the following changes have taken place in 2H-graphite /  $\text{LiCoO}_2$  lithium-ion battery



However, the crystal structure of  $\text{LiCoO}_2$  is the same as that of  $\text{Li}_{1-x}\text{CoO}_2$ , and the latter stay a vacancy in the lattice position of Li. Similar changes have taken place in 2H-graphite/ $\text{Li}(\text{Ni},\text{Co},\text{Mn})\text{O}_2$  lithium-ion batteries as follows



However, the crystal structures of  $\text{LiMeO}_2$  and  $\text{Li}_{1-x}\text{MeO}_2$  are also the same, and the latter stay a vacancy in the lattice position of Li.

The following changes occur during the charging process of 2H-graphite/ $\text{LiFePO}_4$  lithium-ion battery



However, the crystal structures of  $LiFePO_4$ ,  $Li_{1-x}FePO_4$  and  $FePO_4$  are the same, and the phase transition belongs to pseudo-structure phase transition. The latter two are only lack of Li and no Li in the lattice position of Li.

Because of this, we put forward the de-intercalation theory of ionic conductivity of secondary battery, and clarify the conductive mechanism based on the de intercalation theory.

However, the de-intercalation mechanisms of different electrode active materials in secondary batteries are different. The de-intercalation mechanisms of the electrode active materials involved in this paper are summarized as follows:

b) *The deintercalation mechanism of  $\beta\text{-Ni(OH)}_2$*

$\beta\text{-Ni(OH)}_2$  belongs to hexagonal structure, P-3m1 (No.164) space group, there are one molecule in the unit cell, that is, one Ni atom, two oxygen atoms and two hydrogen atoms, a total of five atoms. Their crystallographic positions in the unit cell are as follows:

Atom	position	x	y	z
Ni	1a	0	0	0
H	2c	0	0	$\pm 1/4$
O	2d	$1/3$	$2/3$	$\pm 0.222$

The crystal structure model and chemical bonding are shown in figure 16. As can be seen from the diagram, the chemical bond between Ni and O is stronger, while that between H and O is much weaker. When there is no stacking disorder, the Ni-O layer presses ABAB. The hydrogen is stacked sequentially, and the hydrogen is embedded in two layers between the Ni-O layers. The H atom in  $\beta\text{-Ni(OH)}_2$  has two equivalent positions  $0 0 \pm 1/4$ . The energy required for them to leave the  $\beta\text{-Ni(OH)}_2$  lattice or re-embed into  $\beta\text{-Ni(OH)}_2$  is almost the same, so there is only one charging platform.

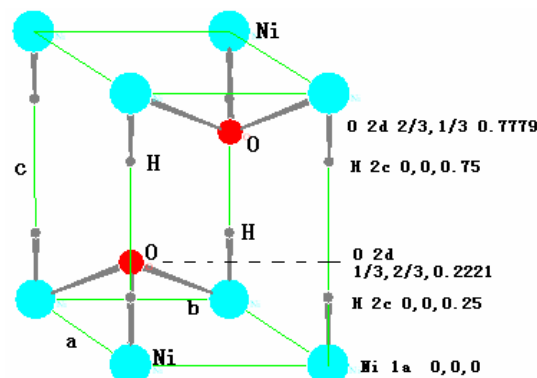


Fig. 16: Crystal structure model and chemical bonding of  $\beta\text{-Ni(OH)}_2$

c) *The de-intercalation mechanism of H in  $AB_5$  alloy*

There is one molecule in the  $LaNi_5$  unit cell, that is, one La atom and five Ni atoms. The crystallographic position of the cell is:

Atom	position	Coordinate
La	1a	0 0 0
Ni-1	2c	$1/3 2/3 0 ; 2/3 1/3 0$
Ni-2	3g	$1/2 0 1/2 ; 0 1/2 1/2 ; 1/2 1/2 1/2$

The crystal structure model and chemical bonding are shown in figure 17.

Before the charging reaches a certain stage, the embedded hydrogen atom occupies the interstitial position of the  $LaNi_5$  lattice and forms the  $AB_5\text{-H}_n$  solid solution. Hydride  $AB_5\text{H}_x$  can be formed only when the cell volume increases to a certain percentage due to the intercalation of hydrogen atoms. Of course, the formation of hydride has a process of nucleation and growth. The discharge process should be a reverse process in which the hydrogen atoms preferentially leave the hydride lattice and gradually decompose the hydride, and then the solid solution hydrogen atoms leave the  $AB_5\text{-H}_n$  solid solution alloy. The maximum value of n is 18. That is that maximum mass fraction of hydrogen storage of  $LaNi_5$  is 1.379%<sup>[30]</sup>.

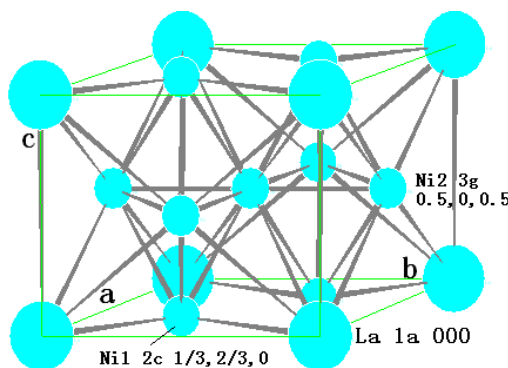


Fig. 17: Crystal structure model and chemical bonding of  $LaNi_5$

d) *Li intercalation mechanism of  $LiMeO_2$  during charge and discharge*

$LiCoO_2$  and  $Li(Ni_{1/3}Co_{1/3}Mn_{1/3})O_2$  both belong to the (No.166) R-3m space group. There are three molecules in the unit cell. 12 atoms, and their occupancy in the cell is:

Li (3a) 000 ;  $2/3 1/3 1/3$  ;  $2/3 1/3 1/3$

Ni,Co,Mn (3b) 001/2 ;  $2/3 1/3 5/6$  ;  $1/3 2/3 7/6$

O (6c) 001/4 ;  $2/3 1/3 7/12$  ;  $1/3 2/3 11/12$  ;  $00-1/4$  ;  $2/3 1/3 1/12$  ;  $1/3 2/3 5/12$

The crystal structure model and chemical bonding are shown in figure 16.

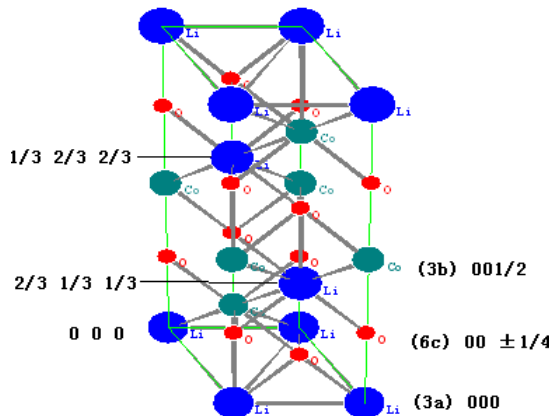


Fig. 16: Crystal structure model and bonding of  $\text{LiMeO}_2$

As can be seen from the diagram, the chemical bond between the Li atom at position 000 and the neighboring atom is longer, and its binding force in the crystal cell is weak. When charging starts, The Li atom at position 000 is preferentially separated from the crystal lattice. The crystal lattice is followed by the Li atom at 2/3 1/3 1/3 ; 2/3 1/3 1/3 position of the crystal lattice, so it is in the charged state. When  $< 30\%$ , the lattice parameters and lattice strain change slowly, and then the rate of change is larger. In the process of discharge, it is roughly the reverse process, but it is not completely reversible.

The appearance of two  $\text{Li}_{1-x}\text{CoO}_2$  with different composition when charging in the range of 10-20% indicates that there is not a uniform de-Li of the whole cathode, but a process from the surface to the inside, and finally achieve a more uniform de-Li of the whole electrode. There is no phase transition during the whole charging and discharging process, but the fine structure (lattice parameters, micro-strain) and relative diffraction intensity, especially (006), of the positive active materials change most obviously due to de-Li and re-embedding Li.

e) *The behavior of  $\text{LiFePO}_4$  material during charge and discharge and the mechanism of Li deintercalation*

Li atoms have four crystallographic positions in the  $\text{LiFePO}_4$  lattice, namely:

000 ; 0 1/2 0 ; 1/2 0 1/2 ; 1/2 1/2 1/2

As can be seen from figure 12, the bonding force at position 000 is the weakest, and the bonding force at position 1/2 1/2 1/2 is the strongest, and that at position 0 1/2 0 is similar to that at position 1/2 0 1/2. Therefore, under the action of a smaller electric field, the Li atom at position 000 first leaves the  $\text{LiFePO}_4$  lattice until it becomes  $\text{Li}_{0.25}\text{FePO}_4$ , and then the Li at position 0 1/2 0 and 1/2 0 1/2 leave successively. Until it becomes Li-deficient  $\text{Li}_{0.50}\text{FePO}_4$  and  $\text{Li}_{0.75}\text{FePO}_4$ , and

finally, the Li atom at position 1/2 1/2 1/2 leaves until it becomes  $\text{FePO}_4$  without Li. There may be four steps in the charge-discharge curve, the difference between the front and the last two steps is large, and the difference between the middle two steps is very small, the discharge process is on the contrary, which is proved by the experimental charge-discharge curve, as shown in figure 15.

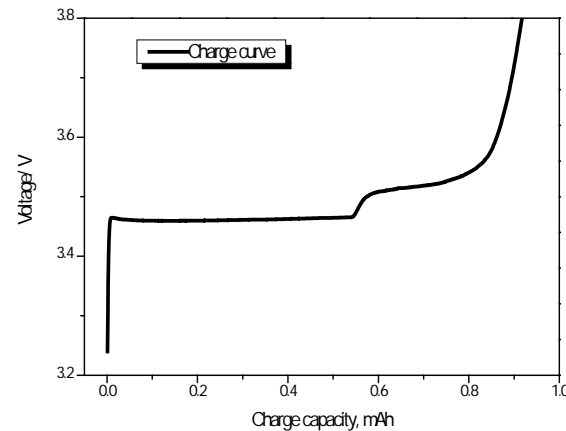


Fig. 15: Charging of Li/LiFePO<sub>4</sub> and its differential curve [29]

f) *Behavior of graphite during charge and discharge*

The structure of graphite is characterized by the extension of the hexagonal grid surface composed of carbon atoms in the network plane and the ABAB along the normal direction of the network plane. Or ABCABC. The former belongs to P63/mmc (No.194) space group and the latter is 3R-graphite and belongs to R3 (No.146) space group [15]. Based on the experimental results of Section 3.2, some behaviors of graphite in the process of charge and discharge can be summarized.

With the beginning of the charging process, the Li atom is embedded in the graphite layer, and its priority is to enter the gap position between the graphite grid faces, so that the lattice parameters  $a$  and  $c$  as well as the micro-strain  $\epsilon$  of the graphite, are increased, and the stacking disorder  $P$  is also changed. Because the ABAB sequential stacking is not as dense as the dense hexagonal structure, it has a large gap space and can hold a large number of interstitial atoms, so the Li-C compound will not be formed when the charge is less than 60%. Only when the battery charge is more than 60%,  $\text{LiC}_{24}$ ,  $\text{LiC}_{12}$ ,  $\text{LiC}_6$  and  $\text{Li}_2\text{C}_2$  phases will be formed successively. Due to the precipitation of the new phase, there is a process of nucleation and growth, so there will be two-phase or polyphase coexistence in this process. As for the percentage of charge in which Li-C compounds are precipitated, it depends on the system of lithium-ion batteries and the proportion of positive and negative active materials.

Similar to the positive electrode, the 002,100 peaks of 2H-graphite are separated when the charge is less than 20%, indicating that there are also two 2H-



graphite phases with different composition, indicating that the graphite electrode also has a surface-to-inside process of embedding Li.

## VI. PHYSICAL MECHANISM OF ELECTRICAL CONDUCTIVITY FOR SECONDARY BATTERY

At the beginning of charging, the migration of lithium ions (hydrogen ions) begins at the negative-electrolyte interface. Because lithium ion (hydrogen ion) is embedded in the negative electrode after obtaining (reducing) electrons at the negative electrode-electrolyte interface, the concentration of lithium ion (hydrogen ion) at the negative electrode-electrolyte interface decreases. In the solution, lithium ion (hydrogen ion) migrates from positive electrode to negative electrode like a relay race to make up for this concentration gap. Due to the directional migration of  $\text{Li}^+$  ions (hydrogen ions), the concentration of  $\text{Li}^+$  ions (hydrogen ions) is also reduced at the positive electrode-electrolyte interface. Under the action of electric field, the Li atoms in positive active materials ( $\text{LiCoO}_2$ ,  $\text{Li}(\text{Ni},\text{Co},\text{Mn})\text{O}_2$ , and  $\text{LiFePO}_4$ ) leave the lattice position (the hydrogen atoms in the  $\beta-\text{Ni}(\text{OH})_2$  leave the lattice position), reach the positive electrode-electrolyte interface, lose electrons (that is, oxidation), and enter the electrolyte. To supplement the lithium ion (hydrogen ion) in the electrolyte. When the ion flow reaches dynamic equilibrium, it corresponds to the charging platform of the battery. When the battery is fully charged, the Li atom (hydrogen atom) in the positive electrode is exhausted, and the  $\text{Li}^+$  ion (hydrogen ion) can only be provided by the electrolyte, so there must be  $\text{Li}^+$  ion (hydrogen ion) in the original composition of the electrolyte.

The discharge process is contrary to the charging process. Under the action of the reverse electric field, the  $\text{Li}^+(\text{H}^+)$  ion in the electrolyte is reduced to atoms at the positive electrode-electrolyte interface and embedded back into the lattice position of the positive active material. Then the  $\text{Li}^+(\text{H}^+)$  ion migrates from the negative electrode to the positive electrode like a relay race, resulting in a decrease in  $\text{Li}^+(\text{H}^+)$  ion concentration at the negative electrode-electrolyte interface. Then the  $\text{Li}(\text{H})$  atom in the negative active material leaves the lattice, loses electrons and becomes  $\text{Li}^+(\text{H}^+)$  ion, which enters the electrolyte through the negative electrode-electrolyte interface, thus forming the discharge conduction process that the negative side  $\text{Li}(\text{H})$  atom leaves the crystal lattice of the negative electrode active material, the positive side  $\text{Li}(\text{H})$  atom is embedded back into the crystal lattice position of the positive electrode active material, and the  $\text{Li}^+(\text{H}^+)$  ion flows directionally from the negative electrode to the positive electrode.

In short, the physical conductive mechanism of secondary battery is the directional migration of conductive ions formed by de-intercalation and re-

intercalation in positive and negative electrode active materials.

## REFERENCES RÉFÉRENCES REFERENCIAS

1. Bode H, Dehmel T K, Witte J. Zur kenntnis der nickelhydrox- idelktode , I. U ber das nickel (II)-hydroxidhydrat [ J ] . *Electrochim Acta*, 1966, 11: 1079~1087.
2. Shukla A.K. Venugopalan S., Hariprakash et al., Nickel-based rechargeable batteries, *J. Power Sources*, 2001, 100:125~148
3. Li Guoxin, Editor-in-Chief, 2007, introduction to New Chemical Power supply Technology (Shanghai: Shanghai Science and Technology Press) 172~218.
4. Xing Zhengliang, Li Guoxun, Wang Chaoqun Xiao Jinsheng, XRD in situ observation of nickel electrode during charge and discharge, *Power supply Technology*, 1999 23 (2): 140~142.
5. Wang Chaoqun, Xing Zhengliang Wang Ning, Li Guoxun, Wu Burong, quantitative Phase Analysis of NiOOH on Nickel electrode, *Power supply Technology*, 1999.
6. Ulrik Palmqvist, Lars Eriksson, Javier Garcia-Garcia et al, On the misuse of the structure model of the Ni electrode material, *J. Powe Source*, 2001, 25(1):15~25
7. Li Yuxia, Yang Chuanzheng, Lou Yuwan, Xia Baojia, study on the physical mechanism of conductivity in the charge-discharge process of MH/Ni batteries, *Journal of Chemistry*, 2009.67 (9): 901-909.
8. Qinpei Lou Yuwan Yang Chuanzheng Xia Baojia, a new method and calculation program for separating multiple broadening effects of X-ray diffraction lines, *Journal of Physics* 2006 55 (3): 1325-1335.
9. Yang Chuanzheng, Zhang Jian some advances in the study of microstructure of nanomaterials by X-ray diffraction, *advances in physics*, 2008, 28 (3): 280.~313.
10. Lou Yu-Wan, Yang Chuan-Zheng, Zhang Xi-Gui et al, Comparative study on microstructure of  $\beta$ - $\text{Ni}(\text{OH})_2$  as cathode material for Ni-MH battery, *Science in China: Series E: Tech. Sci.*, 2006, 49(3):297~312
11. Li Yu-xia (Master thesis of Shanghai Institute of Microsystems and Information Technology, Chinese Academy of Sciences): research on the relationship between the fine structure of electrode active materials and the function of Ni/MH batteries. P.53.
12. Yang Chuanzheng, Lou Yu-Wan, Li Yuxia, Xia Baojia, some advances in the study of the relationship between the performance of Ni/MH batteries with fine structure of electrode active materials, *advances in Physics*, 2009, 29 (1): 109, 126.

13. Reimers JN and Dahn JR, *J. Electrom. Soc.*, 1992, 139(8):2091~2096.
14. Amatucci G G, Taracín J M and Klein L C, *J. Electrochem. Soc.*, 1996, 143(3):1114~1123.
15. Yang XQ, Sun X, McBreen J, *Electrochem. Commun.*, 2000, 2:100~103
16. Sun X, Yang XQ, McBreen J, et al., *J. Power Sources*, 2001, 97-98:274~276
17. Li Jia, Yang Chuanzheng, Zhang Jian, Zhang Xigui, Xia Baojia, *Journal of Chemistry*, 2010 pr 68 (7): 646 ~652.
18. Li Jia, Yang Chuanzheng, Zhang Jian, Xia Baojia, *Journal of Physics*, 2009 58 (9): 6573~6581
19. Padhi A.K., Nanjundaswamy K.S. Goodenough J.B., *J. Electrochem. Soc.* 1997, 144:1188,
20. Srinivasan V., Newman J., Discharge model for the lithium iron-phosphate-electrode, *J. Electrochem. Soc.*, 151(10): A1517-A1529
21. Yamada A., Koizumi H, Sonoyama N., Kanno R., Phase change in  $\text{Li}_x\text{FePO}_4$ . *Electrochem. Solid-State Letters*.2005, 8(8): A409-A413
22. Dodd J.L., Yazami R., Fultz B., Phase diagram of  $\text{Li}_x\text{FePO}_4$ , *Electrochem. Solid-State Letters*, 2006, 9(3): A151-A155
23. Qian Wang, Jian Zhang, Chuan-Zheng Yang, Bao-Jia Xia, *J. Electrochem. Soc.*,
24. Liu Haohan, Li Jia, Zhang Jian, Yang Chuanzheng, Xia Baojia, Phase transition Nature and Conductive Mechanism of Graphite /  $\text{LiFePO}_4$  Battery during charge and discharge, 2010, to be published
25. Destenay D., *Mem.Soc. Roy. Sci.*, 1948,10(4)28; Wilson A.J.C., *Structure Reports*, 1950,13:319
26. Eventoff W, Martin R and Peacor D.R., *Amer.Min.*, 1972,57:45~51 ; *Structure Reports*,1972,38A:314
27. Zhang Jian, Wang Qian, Xie Xiaohua, Yang Chuanzheng, Xia Baojia, strain Analysis and Conductive Mechanism of Lithium Ion Battery during charge and discharge, *Journal of physical Science*, 2012jue 1 (1): 72~86.
28. Jiang Chuanhai, Yang Chuanzheng, Internal stress diffraction Analysis, Chapter 14 stress Analysis and Conductive Mechanism of Green Secondary Battery Beijing: science Press, 2013.11.
29. Yang Chuanzheng, Lou Yuwan, Zhang Jian, Xie Xiaohua, Xia Baojia, material characterization and electrode process Mechanism of Green Secondary Battery, *Science Press*, 2015.9.
30. Yang Chuanzheng, study on Kinetic characteristics and Mechanism of hydrogen absorption/Desorption of Alloy hydrogen Storage Materials, *material Science*, 2020 ~ (12): 1002 ~ 1026
31. Yang Chuan-Zheng, Lou Yu-Wan, Zhang Jian, Xie Xiao-Hua and Xia Bao-Jia, «Characterization of Material and Mechanism of electrode process for green secondary Battery», *Science Press Beijing*, 2015
32. Chuan-Zheng Yang, Yu-Wan Lou, Jian Zhang, Xiao-Hua Xie and Bao-Jia Xia, «Materials and Working Mechanisms of Secondary Batteries», Springer, *Science Press in Beijing*, 2022.

Table 1

Materials and Working Mechanisms of Secondary Batteries	
Authors	C. Z. Yang, Y. W. Lou, J. Zhang, X. H. Xie and B. J. Xia
Publisher	Springer and Science Press in Beijing
Content synopsis	<p>This book is a monograph on material characterization and the mechanism study during charge-discharge, cycle and storage for secondary batteries by X-ray diffraction et al methods. whole book consists of 6 parts and 21 chapters. Part. 1(chap.1,2) describes the key experimental techniques and data analysis methods of X-ray diffraction. Part.2 (Chap.3~8) introduces the preparation methods and X-ray diffraction characterization of electrode active materials, including <math>\beta\text{-Ni(OH)}_2</math>, storage hydrogen alloy <math>\text{AB}_5</math>, <math>\text{LiMeO}_2</math>, <math>\text{LiFePO}_4</math> and 2-H graphite.etc al. In this two parts, several new methods have been developed:(1) The least square method of separating the multiple broadening effect of diffraction lines and program for solving microstructure parameters; (2)A solution of mixed occupation parameters for Ni/Li atoms at 3a and 3b crystallographic sites of materials such as <math>\text{LiNiO}_2</math>, <math>\text{Li}(\text{Ni},\text{Co})\text{O}_2</math>, <math>\text{Li}(\text{Ni},\text{Mn})\text{O}_2</math> and <math>\text{Li}(\text{Ni},\text{Co},\text{Mn})\text{O}_2</math>; (3) A new technique for measuring the stacking disorder of hexagonal graphite.</p> <p>Part 3 (Chap.9~12) introduces the mechanism studies during charging and discharging for (Ni/MH), graphite/<math>\text{LiMeO}_2</math> and graphite/<math>\text{LiFePO}_4</math> batteries. Based on the phase transition theory, a new intercalation-de-intercalation theory and conduction mechanism of conductive ions are proposed; Part 4 (Chap.13~16) and part 5 (Chap.17~19) are the mechanism study of the of cycle process and storage process, respectively. In these two parts, through the comparative study of variation laws of battery performance and of fine structure and microstructure parameters of positive and negative active materials and diaphragm with cycle and storage process, the cycle and storage processes mechanism and battery performance decay mechanism are revealed; Part 6 (Chap.20 and 21) investigates the methods to improve the battery performance based on the understanding of decay mechanism of cycle and storage performances of batteries</p> <p>The research methods, contents and new results introduced in the book fully reflect the necessity and importance of interdisciplinary intersection and close cooperation between material physics and</p>



electrochemistry, X-ray diffraction analysis and battery experts in this kind of research.		
Chapter	Chapter Name	page
0	Preface, Catalogue and the author's introduction	38
1	Experimental methods of material characterization and the mechanism research	1
2	X-ray Diffraction analysis Methods of Materials Characterization and Mechanism Research	23
3	Characterization of active material $\beta$ -Ni(OH) <sub>2</sub> and AB <sub>5</sub> alloy	61
4	Solid state reaction and formation mechanism in the synthesis of LiMeO <sub>2</sub> materials.	83
5	Mixed Occupation of Ni/Li Atoms in LiMeO <sub>2</sub> Materials	99
6	Ordered-Disordered of Ni, Co and Mn in (3b) position for Li(Ni <sub>1/3</sub> Co <sub>1/3</sub> Mn <sub>1/3</sub> )O <sub>2</sub>	121
7	Preparation and X-ray Diffraction Characterization of LiFePO <sub>4</sub>	139
8	Preparation and X-ray analysis of carbon electrode materials for lithium-ion batteries	159
9	Solid electrolyte Interface Film on Graphite Surface of Lithium-Ion Battery	207
10	Mechanism Research of Charge-discharge Process for MH/Ni Battery	227
11	Mechanism of charge-discharge process of Graphite/LiCoO <sub>2</sub> and Graphite/Li(Ni <sub>1/3</sub> Co <sub>1/3</sub> Mn <sub>1/3</sub> )O <sub>2</sub> batteries	247
12	Mechanism Research of Charge-Discharge Process for Graphite/LiFePO <sub>4</sub> battery	275
13	Mechanism Research of Cycle Process for MH/Ni Battery	297
14	Mechanism Research on the Cycle Process of 2H-Graphite/Li(Ni,Co,Mn)O <sub>2</sub> Battery	315
15	Cycle mechanism of graphite/[Li(Ni <sub>0.4</sub> Co <sub>0.4</sub> Mn <sub>0.4</sub> )O <sub>2</sub> +LiMn <sub>2</sub> O <sub>4</sub> ]	339
16	Mechanism of Cycle Process of Graphite/LiFePO <sub>4</sub> Battery	351
17	Mechanism research of Storage Process for MH-Ni Battery	365
18	Mechanism of Storage Process for Graphite/LiCoO <sub>2</sub> and Graphite/Li(Ni <sub>1/3</sub> Co <sub>1/3</sub> Mn <sub>1/3</sub> )O <sub>2</sub> batteries	379
19	Mechanism Research of Storage process for Graphite/LiFePO <sub>4</sub> Battery	417
20	Effect and Action Mechanism of $\beta$ -Ni(OH) <sub>2</sub> Additive in MH/Ni Battery	443
21	The Method and Action Mechanism of Improving the Performance of Secondary Battery	461
The recommendation of three professorial experts		491
Subject index		495
The sum of the whole book		497 + 38 = 535